2020 17th International Conference on Electrical Engineering, Computing Science and Automatic Control (CCE).
Mexico City, Mexico. November 11-13, 2020

Detection of Sore-risk Regions on the Foot Sole with Digital Image Processing and Passive Thermography in Diabetic Patients

Rafael Bayareh Mancilla
Department of Electrical Engineering/Bioelectronics, CINVESTAV-IPN
Université de Lorraine - CRAN-BioSiS
Mexico City, Mexico - Nancy, France
rafael.bayareh@cinvestav.mx

Christian Daul
Université de Lorraine/CNRS, CRAN-BioSiS
Nancy, France

Josefina Gutierrez Martínez
INR-LGII, Direction of Technological Research, Medical Engineering Research Division
Mexico City, Mexico

Arturo Vera Hernández
Department of Electrical Engineering/Bioelectronics, CINVESTAV-IPN
Mexico City, Mexico

Didier Wolf
Université de Lorraine/CNRS, CRAN
Nancy, France
didier.wolf@univ-lorraine.fr

Lorenzo Leija Salas
Department of Electrical Engineering/Bioelectronics, CINVESTAV-IPN
Mexico City, Mexico
lleija@cinvestav.mx

Abstract — **According to the International Diabetes Federation, approximately four million people die from diabetes each year, and ten million more suffer disabling or potentially terminal complications, such as diabetic foot disease. Therefore, the proposal is the early detection by detecting non-homogeneous temperature regions with radiometric data and image processing by IR thermography. The samples were taken from 12 patients diagnosed with diabetes mellitus without a history of diabetic foot or visible anatomical alterations, by a cooled IR sensor programmed exclusively to measure human skin temperature. The radiometric data was processed to eliminate interferences and segment the lower limb since the acquisition was carried out in a non-controlled environment; where lies the relevance of this paper. The results were presented as binary images with a defined segmented region against a contrasting background, reviling areas corresponded to higher temperatures regard the rest of the sole fo the foot as a consequence of non-homogeneous temperature pattern. A total of 6 cases showed a normal homogeneous temperature, 2 cases had fault origins and 4 cases presented spotted regions that are prospective to prone lesions. This procedure set a precedent for the analysis of early detection of the diabetic foot with radiometric data processing instead of using IR images as input; which could be used to retrieve the coordinates and carry out an exhaustive numerical analysis or pattern recognition (i.e. thermal fingerprint) to support the anticipated diagnosis based on support systems such as medical thermography as perspective.**

Keywords — Diabetic foot, IR medical thermography, image processing.

I. INTRODUCTION

According to the International Diabetes Federation, four million people die from Diabetes Mellitus (DM) each year and dozens of millions more suffer disabling and potentially fatal complications, such as lower limb amputation as a result of diabetic foot (DF) disease in which is related to infectious diseases and death [1]–[4]. Consequently, the diabetic foot complication is often a threat for patients with Diabetes Mellitus since it is a consensus to amputate below the knee joint as a preventive measure, in which often anticipated diagnosis receives limited attention and research [5]–[7].

Early diagnosis and treatment of the DF are related to understanding the physiology from a detectible and quantitative point of view. A modern and popular method for pre-diagnose certain illnesses including DF is medical IR thermography, which is a contactless, non-invasive technique to measure superficial temperature [7]–[9]. The principle of medical IR thermography is the indirect measurement of temperature as the interpretation of the IR radiation emitted by a body with heat. These data allow different analyses such as temperature differences in regions as a quantitative indicator of a complication such as DF [10]. However, the approval of IR thermography as an acceptable standardized procedure is still under the research stage by the medical community due to the importance of quantification of clinical data, understanding the nature of thermal images and training image acquisition and interpretation [8]. Several studies have concentrated their efforts on proving the concept and systematic application of medical thermography. Table 1 describes the state of the art regarding image processing applied for the identification of risk zones in the diabetic foot.

Table 1: Overview of the state of the art of IR thermography related to diabetic foot illness.

Author	Year	Instrument	Algorithm input	Detection
Vilcahuaman [11]	2014	FLIR i5	IR images	Temperature of the plantar foot.
Liu [12]	2016	FLIR i5	IR images	Diabetic Foot Hyperthermia.
Kaczmarek [9]	2016	Unspecified	IR images	Wound healing identification.
Fraiwan [13]	2017	FLIR ONE	IR images	Diabetic foot ulcer.

The studies described in Table 1 have in common that the input of their algorithms are IR images. This paper explores the perspective processing radiometric data to obtain a delimited IR image without interferences when there is no possibility to have a controlled environment, so the results would integrate IR thermography and image processing for the cutaneous temperature discrimination threshold for early DF diagnosis. However, some uncontrolled conditions are above the limits of the algorithm proposed in this paper which will be overview in

978-1-7281-8987-1/20/$31.00 ©2020 IEEE

further sections. Section II describes in detail the methodology setup, IR technology, and the image processing technique. Section III explains the obtained results as this manuscript concludes as a possible technique to detect high-risk zones to develop lesions or ulcers as a precedent for the study of diabetic foot early diagnosis.

II. METHODS

A. Participants and protocol acquisition

The study was conducted in collaboration with the National Rehabilitation Institute - Luis Guillermo Ibarra Ibarra, Mexico; where consent forms were provided to each of the volunteers.

Samples were taken from 12 patients diagnosed with DM without a clinical history of DF or visible anatomical alterations or inflammation. The range of ages was between 41 and 81 years, with 24 years to 1 year with DM diagnosis, no visible alteration or deformation on the lower limbs nor discomfort, 83% where female patients, and 13% male. Each volunteer was placed in supine position. The lower limb was left to cool for 10 minutes as suggested in the passive thermography technique [14]. After the temperature homogenization process, the thermographic equipment was set up at 20 cm regard to the sole of the foot as illustrated in Fig. 1.

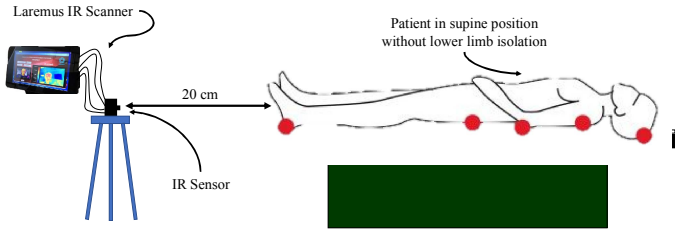

Fig. 1: Experimental setup diagram

B. Instrumentation setup

The thermographic equipment is a prototype developed in a past project using an embedded system in which results and validation were presented by Bayareh et al [15]. The design and programming had a purpose to read human skin temperature and retrieve thermal maps and images under a mathematical model that predicted the superficial temperature as an indirect measurement of IR longwave energy [16]. Table 2 summarizes the thermal imager technical characteristics.

Table 2: Lepton 2.5 LWIR thermal imager

Characteristics	Range	Units
Infrared sensor resolution	80 x 60	Pixel
Pixel size	17	µm
Thermal Sensitivity	≤ 50	mK
Infrared Spectral Band	8 – 14	µm
Voltage	2.8	V
Refresh rate	8.6	FPS

The retrieved thermal map can be processed as a double type data array, in which the following section describes the data treatment, color mapping and image reconstruction.

C. Data analysis

The input parameters for the algorithm is a radiometric array retrieved from the IR sensor, composed of 14-bit values and structured by 60 x 80 size. Each radiometric array is possible to process, analyze and segment as much as possible the region of interest (ROI) respect the background and eliminate any non-desirable artifacts. A fundamental advantage of thermography is that the measured object usually is hotter or colder regard to the background [18]. In such a way, the values of the ROI could be separate and analyze the information inside the delimited region.

The first step was to organize the data by range normalization from 0 to 1 (equation 1). After, the data arrays were sorted by a high pass filter set to 80%, so that low values were transformed to be part of the background as equation 2 describes and Fig. 2 illustrates the concept.

$$f(x) = \frac{x - min(x)}{max(x) - min(x)} \tag{1}$$

$$f(x) = \begin{cases} x, & x > 0.8 \\ 0, & x < 0.8 \end{cases} \tag{2}$$

Where x represents the value in each paired location of the matrix.

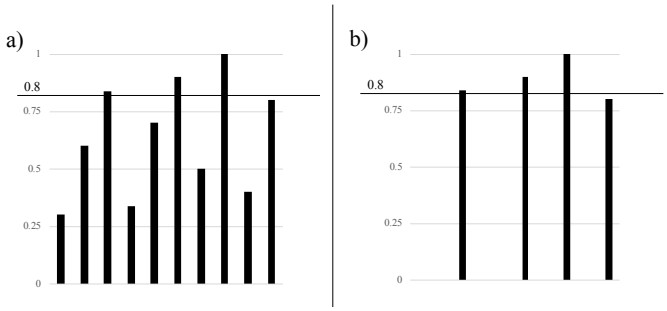

Fig. 2 a) illustrated the original values input, meanwhile b) shows the filter effect in which only values higher than 0.8 were kept and the rest were changed to zero.

Once the processed array was achieved, it was mapped into a scale color in order to reconstruct an RGB image out of sorted data. A simple example of this resulted image is given by Fig. 3. This concept is homologous to the definition of an image given as a binomial function $f(x,y)$ associated with an intensity described by Gonzales and Woods [17].

Fig. 3: Mapped values into a colored image with a Jet color scale (64 tones). Given a matrix 3x3 composed of consecutive numbers from 1 to 9. Each value is sorted from low to high, being blue assigned to the lowest value and red to the highest value.

After the mapping procedure, the images were processed by image processing techniques to detect the samples with intensity values that are associated with abnormal temperature behavior in the sole of the foot. Each image was converted into grayscale by forming a weighted sum of the R, G, and B components; the coefficients used to calculate grayscale values are identical to those used to calculate luminance in Rec.ITU-R BT.601-7 standard after rounding to 3 decimal places [19], as equation 3 describes.

$$f_G(x) = 0.299 \cdot \mathrm{R} + 0.587 \cdot \mathrm{G} + 0.114 \cdot \mathrm{B} \qquad (3)$$

Where R, G and B are the color 8-bit scale component of each pixel.

When image coordinates (*x,y*) and its associate intensity are discrete values, this can be considered as a digital image. Thus, each image was binarized for contrast cutaneous temperature by a threshold technique, i.e. Otsu threshold method [20]. Fig. 4 shows an example of the Otsu threshold transformation.

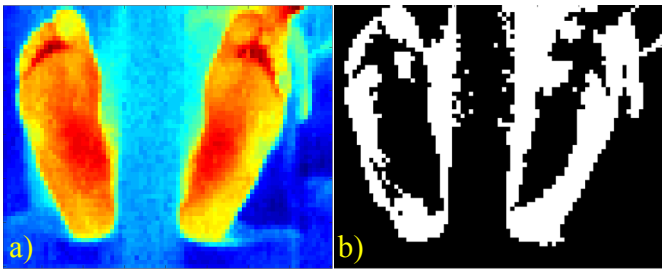

Fig. 4: a) IR raw image out of the sensor while b) is the corresponding binarize image with an Otsu threshold of 64%.

As Fig. 4 b) displays, a binary image can be consistently obtained from the calculated threshold. In such a way, several regions can be detected by retrieving the coordinates if they are connected by neighbor pixel and well isolated. If several regions are connected, it can be applied to an erosion process to separate each region. Equation 4 describes the erosion process by an inverted structuring element neighborhood mask [21].

$$A \ominus B = \{Z | (Bz \subseteq A\} \qquad (4)$$

$$\mathrm{B} = \begin{pmatrix} 1 & \cdots & 1 \\ \vdots & X & \vdots \\ 1 & \cdots & 1 \end{pmatrix}, X = \begin{bmatrix} 0 & 0 & 0 \\ 0 & 1 & 0 \\ 0 & 0 & 0 \end{bmatrix}$$

Where A is a binary image, B is the structuring element, Bz is the translation of B by the vector Z over the image A.

The structuring element can be defined by the user depending on the applications and results. For this particular task, B was defined as a square matrix of 13x13 elements with a center X due to the best erosion result. The relevance of eroding the binary images is to delimit the possible areas of interest and to separate a group of pixels that at first results as a single entity as shown in Fig. 5-a).

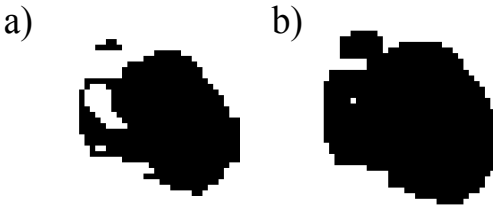

Fig. 5: a) binarized image after Otsu transformation threshold with three regions, b) Eroded binary image with two regions where the biggest correspond to the background which is discarded as a region of interest.

Afterward, the areas were detected by 4-connected regions described by equation 4 and illustrated in Fig. 6.

$$f(x,y) \exists \begin{cases} f(x \pm 1, y) = 1 \\ f(x, y \pm 1) = 1 \end{cases} \qquad (4)$$

Where a pixel with coordinates x, y is a 4-connected pixel it the consecutive upper, downer, left or right pixel exists [22].

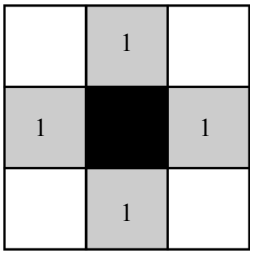

Fig. 6: Example of 4 connectivity pixels, which are neighbors to every pixel that contacts one of their edges and are connected vertically and horizontally.

The processes described above allow delimiting an area of interest according to the intensity of color as it is indirectly proportional to the areas with non-homogeneous temperatures in the plant area. As a final point, also this technique allows finding the coordinates of a relevant area to be segmented in a later process in order to investigate the difference of temperature or patterns in the thermal footprints. Fig. 7 illustrates briefly the process described in this section.

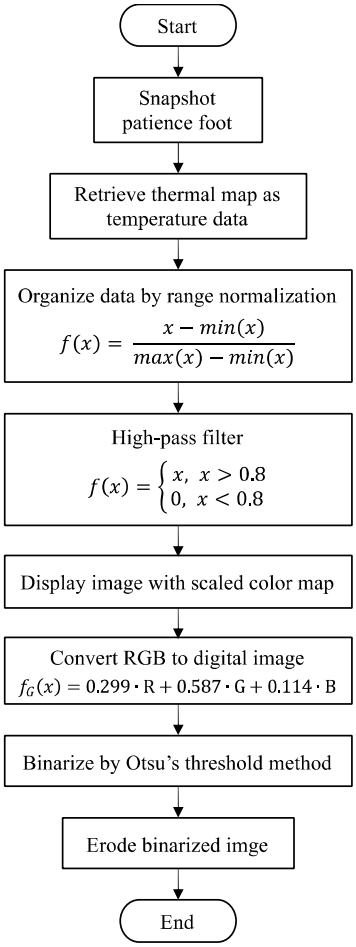

Fig. 7: Flow chart for detect high-risk zones to develop ulcers in the sole of the foot by temperature differences

III. Results

The results are presented as binary images with a defined segmented region against a contrasting background, reviling areas corresponded to higher temperatures regard the rest of the sole fo the foot as a consequence of non-homogeneous temperature pattern. A total of 6 cases showed a normal homogeneous temperature, 2 cases had fault origins and 4 cases presented spotted regions that are prospective to prone lesions. Fig. 8 shows the cases where was detected non-homogeneous temperature values, which is indirectly related to develop lesions. It is important to reach out that the regions detected are in areas that are typically susceptible to developing diabetic foot injuries [23]. The relevance of acquiring snapshots without IR interference and adequate distance is that the algorithm can recognize and filter the background of the ROI.

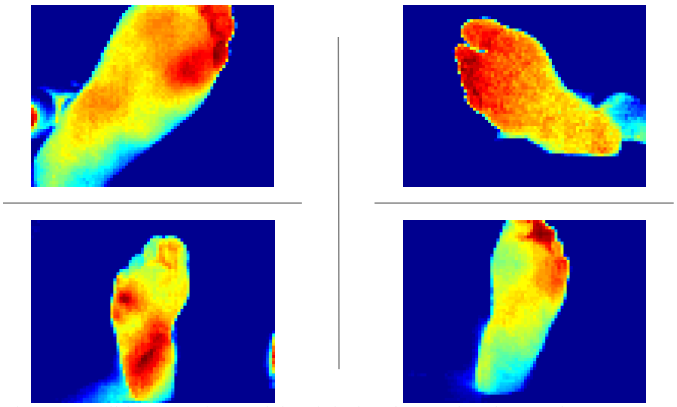

Fig. 8: Possible cases for evolving injuries due to the abnormal temperature pattern.

However, six patients did not show abnormal temperature patterns as presented in Fig. 9. The temperature on the sole of the foot was homogeneous after setting the foot with ambient temperature for 10 minutes.

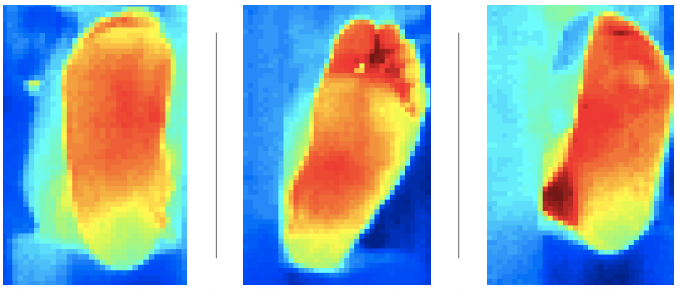

Fig. 9: Cases where patients did not present abnormal temperature differences to be detected by the proposed algorithm.

Nevertheless, two cases had origin errors due to IR interferences and protocol acquisitions under non controlled environment. Fig. 10 illustrates the result of these faults.

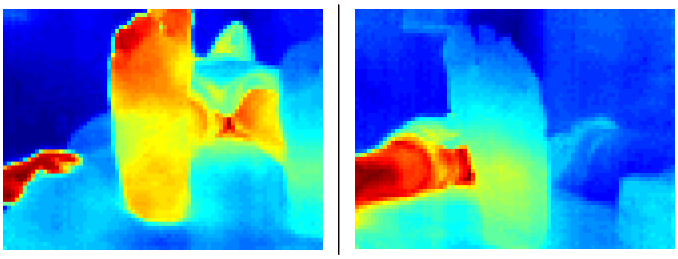

Fig. 10: Origin faults due to IR interferences such as higher temperature regions that opaque the region of interest.

Once the positive cases were detected, the images where to binarize to detect as first approximation a possible high-risk region as displayed in Fig. 11. The threshold was determined automatically by the Otsu method.

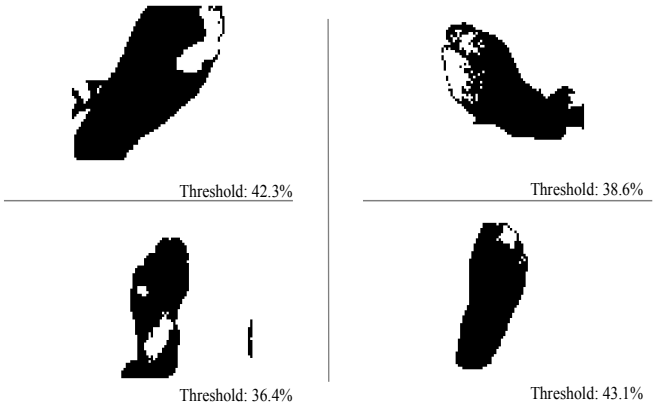

Fig. 11: Binarized images by Otsu's threshold method. The white islands inside the sole region are clustered in multiple regions due to the lack of pixels connectivity.

Due to the lack of connectivity between pixels in the regions of interest, it was necessary to erode the image in order to unify all those pixels that lack connectivity or small islands that are not representative of the problem. The results are displayed in Fig. 12.

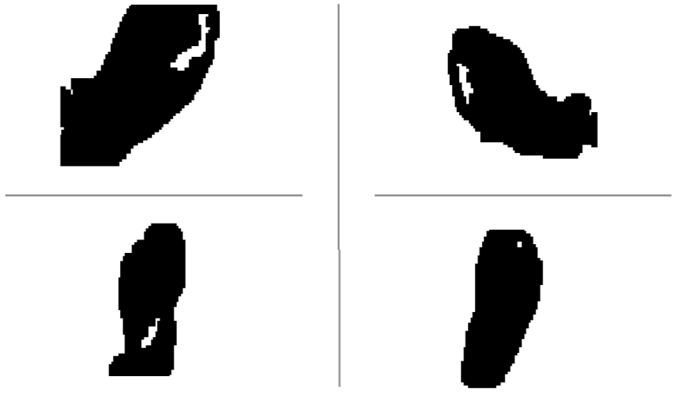

Fig. 12: Eroded images with enclosed regions related to abnormal temperature and injury risk.

IV. Discussion of Results

Although the cases detectable represent 30%, the results show that the algorithm can be a reliable technique to detect areas that may represent a risk to develop injuries in terms of non-homogeneous temperature behavior represented as gray intensity levels.

By defining these regions, it is possible as a perspective to retrieve the coordinates of the area of interest in order to analyze quantitatively such as temperature difference or pattern recognition of thermal fingerprints at the early stage of the complication as further applications. Although within the scope of the results, the algorithm only detects one region per sample, it will be necessary to implement a modification in the erosion stage to detect multiple instead of a single area.

Eventually, it may necessary to perform an exhaustive test to a larger number of patients and samples in order to carry out statistical analysis to support the main hypothesis; anticipate de diabetic foot complication by abnormal temperature behavior study.

V. Conclusions

The proposed algorithm proved the feasibility to detect non-homogeneous temperature zones in terms of gray levels with digital image processing techniques represented as binary images with defined islands on the sole, whose regions are segmented against a contrasting background as a proportional relation to radiometric measurement. Although not all patients exposed a non-homogeneous temperature pattern on the sole or had origin faults, it was possible to detect at least 4 cases that had considerable temperature differences so that the Otsu threshold segmentation stage could reveal regions with a higher temperature than the rest of the sole area and are commonly disposed to prone lesions. However, these zones were not defined in the first stages as a single connected region, so it was necessary to erode in order to merge the granulated scattered pixels and reduce the area to a specific zone. Though the temperature difference is not known as a numerical data at this point, patients with non-homogeneous temperature proved to be a possible symptom for developing diabetic foot at the early stage of the Meggit-Wagner classification. Nevertheless, more robust techniques must be applied for multiple, precise and shaped detection of the regions of interest by retrieving their precise coordinates and provide further quantitative analysis of the region.

The contribution of this work lies in segmenting the plantar zone of the background through the processing data of radiometric information, the elimination of interference from the sole In this way, it is possible to isolate the region of interest and analyze the sole in search of thermal patterns and detection of zones with abnormal temperature behavior with computer vision techniques; that would indicate a possibility to prone injuries or develop diabetic foot. In this sense, the proposed algorithm when is not possible to ensure a controlled environment that allows isolating the lower limb from IR interferences such as a lamp, thermal shadows or even the patient body parts. Given this limitation, the radiometric data processing is a solution when classification with a database or other more complex image processing techniques is not available.

This procedure set a precedent for the analysis of early detection of the diabetic foot complication to be applied in computational tools that allow a more comprehensive and quantitative study in diabetic patients, in terms of processing radiometric data instead of an IR image as input. The recovered data could be used as a perspective for an exhaustive numerical analysis or pattern recognition (i.e. thermal fingerprint) to support the anticipated diagnosis based on support systems such as medical thermography; despite an extensive sample taking and statistical analysis in diabetic patients. Also, the importance of extracting numerical data from IR sensors supports the outlook of reconstructing an RGB image as an indirect

measurement of temperature; so the gray levels of a digital image have a temperature direct correlation; which this information supports diagnosis criteria.

ACKNOWLEDGMENT

We appreciate the funding for the development of the work presented project: CYTED-DITECROD-218RT0545 and Proyecto IV-8 call Amexcid-Auci 2018-2020.

Special thanks to MSAM. Tấn Bình Phan, MSc. José Hugo Zepeda Peralta and MSc. Rubén Pérez Valladares for their collaboration and contribution in this work.

REFERENCES

[1] Federación Internacional de Diabetes, "Plan Mundial Contra la Diabetes 2011-2021," *Fed. Int. Diabetes*, p. 28, 2011.

[2] T. Loaeza Ramos and V. A. Morales Ortiz, "Epidemiología , diagnóstico y tratamiento de la Diabetes Mellitus tipo 2 en niños y adolescentes," *Temas Cienc. y Tecnol.*, vol. 18, no. 54, pp. 3–10, 2014.

[3] International Diabetes Federation, *Diabetes Atlas de la FID*. 2017.

[4] R. F. M. van Doremalen, J. J. van Netten, J. G. van Baal, M. M. R. Vollenbroek-Hutten, and F. van der Heijden, "Infrared 3D Thermography for Inflammation Detection in Diabetic Foot Disease: A Proof of Concept," *J. Diabetes Sci. Technol.*, vol. 14, no. 1, pp. 46–54, 2019.

[5] A. Bhargava, A. Chanmugam, and C. Herman, "Heat transfer model for deep tissue injury: A step towards an early thermographic diagnostic capability," *Diagn. Pathol.*, vol. 9, no. 1, pp. 1–18, 2014.

[6] L. V. Fortington, J. H. B. Geertzen, J. J. Van Netten, K. Postema, G. M. Rommers, and P. U. Dijkstra, "Short and long term mortality rates after a lower limb amputation," *Eur. J. Vasc. Endovasc. Surg.*, vol. 46, no. 1, pp. 124–131, 2013.

[7] B. B. Lahiri, S. Bagavathiappan, T. Jayakumar, and J. Philip, "Medical applications of infrared thermography: A review," *Infrared Phys. Technol.*, vol. 55, no. 4, pp. 221–235, 2012.

[8] N. A. Diakides, M. Diakides, J. Lupo, J. L. Paul, and R. Balcerak, "Advances in medical infrared imaging," in *Medical Devices and Systems*, 2006, pp. 19-1-19–14.

[9] M. Kaczmarek and A. Nowakowski, "Active IR-Thermal Imaging in Medicine," *J. Nondestruct. Eval.*, vol. 35, no. 1, pp. 1–16, 2016.

[10] K. Otsuka, S. Okada, M. Hassan, and T. Togawa, "Imaging of skin thermal properties with estimation of ambient radiation temperature," *IEEE Engineering in Medicine and Biology Magazine*. 2002.

[11] L. Vilcahuaman, R. Canals, M. L. Zequera, and C. Wilches, "Detection of diabetic foot hyperthermia by infrared imaging Automatic Analysis of Plantar Foot Thermal Images in at-Risk Type II Diabetes by Using an Infrared Camera," no. July 2015, 2014.

[12] Y. Liu *et al.*, "Detection of diabetic foot hyperthermia by using a regionalization method, based on the plantar angiosomes, on infrared images," in *Proceedings of the Annual International Conference of the IEEE Engineering in Medicine and Biology Society, EMBS*, 2016.

[13] L. Fraiwan, M. AlKhodari, J. Ninan, B. Mustafa, A. Saleh, and M. Ghazal, "Diabetic foot ulcer mobile detection system using smartphone thermal camera: A feasibility study," *Biomed. Eng. Online*, vol. 16, no. 1, pp. 1–19, 2017.

[14] I. Grubišić, L. Gjenero, T. Lipić, I. Sović, and T. Skala, "Active 3D scanning based 3D thermography system and medical applications," in *MIPRO 2011 - 34th International Convention on Information and Communication Technology, Electronics and Microelectronics - Proceedings*, 2011, pp. 269–273.

[15] R. Bayareh, A. Vera, L. Leija, and J. Gutierrez-Martínez, "Development of a thermographic image instrument using the raspberry Pi embedded system for the study of the diabetic foot," *I2MTC 2018 - 2018 IEEE Int. Instrum. Meas. Technol. Conf. Discov. New Horizons Instrum. Meas. Proc.*, pp. 1–6, 2018.

[16] R. Bayareh-Mancilla, A. Vera-Hernández, L. Leija-Salas, A. Ramos, and J. Gutierrez-Martínez, "Characterization of a Longwave infrared imager for the telemetric measurement of human skin temperature of diabetic foot," *Pan Am. Heal. Care Exch. PAHCE*, vol. 2017-March, pp. 70–74, 2017.

[17] R. C. Gonzalez, R. E. Woods, and B. R. Masters, "Digital Image Processing, Third Edition," *J. Biomed. Opt.*, 2009.

[18] E. Edis, I. Flores-Colen, and J. De Brito, "Passive thermographic detection of moisture problems in façades with adhered ceramic cladding," *Constr. Build. Mater.*, 2014.

[19] International Telecommunication Union Radiocommunication Sector (ITU-R), "Studio encoding parameters of digital television for standard 4:3 and wide screen 16:9 aspect rations," *Recomm. ITU-R BT.601-7*, vol. 7, pp. 2–8, 2011.

[20] N. Otsu, "THRESHOLD SELECTION METHOD FROM GRAY-LEVEL HISTOGRAMS.," *IEEE Trans Syst Man Cybern*, 1979.

[21] R. C. Gonzalez, R. E. Woods, and S. L. Eddins, "Digital Image Processing Using Matlab - Gonzalez Woods & Eddins.pdf," *Education*. 2004.

[22] A. Rosenfeld and J. L. Pfaltz, "Sequential Operations in Digital Picture Processing," *J. ACM*, 1966.

[23] Health Institute for preventive diabetic foot, "Neuropathy / Numbness." [Online]. Available: https://www.ipfh.org/foot-conditions/foot-conditions-a-z/neuropathy-numbness.